Mesomechanics 2009

The influences of multiscale-sized second-phase particles on fracture behaviour of overaged 7000 alloys

Z. Cvijović[a],*, M. Vratnica[b], I. Cvijović-Alagić[c]

[a]Faculty of Technology and Metallurgy, University of Belgrade, Karnegijeva 4, 11120 Belgrade, Serbia
[b]Faculty of Metallurgy and Technology, University of Montenegro,Cetinjski put b.b., 81000 Podgorica, Montenegro
[c]Institute of Nuclear Sciences "Vinča", P.O. Box 522, 11001 Belgrade, Serbia

Abstract

To identify the most important parameters of multiscale microstructural features influencing the fracture modes and resistance to damage, detailed microstructural and fractographic analysis of overaged 7000 alloy plates are performed using the broken plane-strain fracture toughness, K_{Ic}, test specimens. The geometric characteristics of differently sized second-phase particles are changed by the compositional variations. It was found that the fracture process involves three main micromechanisms. The dominant fracture mode changes with alloy purity, leading to fracture toughness degradation. Quantitative description of fractures by profilometry confirmed that crack initiation and propagation is fostered by the coarse Fe- and Si-rich particles.

1. Introduction

The fracture toughness of high-strength 7000 alloys is a critical parameter, limiting their utilisation for highly stressed structural parts[1,2]. The mechanical properties of many materials observed at the macroscopic scale depend on microstructure, often containing multiscale features. In heat-treatable aluminium alloys they are mainly associated with the multiscale-sized second-phase (SP) particles. Their sizes span a length-scale of over three orders of magnitude. All types of these differently sized SP particles make significant contributions to the fracture process and then in determining the mechanical responses[1-4]. As a result, the fracture process in wrought products of commercial aged 7000 alloys involves multiple micromechanisms[1,3,4]. The fracture toughness level is dependent on the relative contributions of these micromechanisms to the overall fracture. Therefore, quantitatively understanding how multiscale features exert their influences on fracture mechanisms and resistance to damage is very rewarding.

Namely, the ability to provide a quantitative description of material behaviour that can be used in continuum calculations is central for developing advanced aluminium alloys. The most effective approach to construct a multiscale model, in which quantitative relations are revealed between fracture toughness and the parameters of

_____

* Corresponding author. Tel.: +381-11-3370-469; fax: +381-11-3370-387.
E-mail address: zocvij@tmf.bg.ac.rs (Z. Cvijović).

these multiscale microstructural features, is to display explicitly the independent influence and to analyse the coupled influence from every population of SP particles. To fulfil this task, the initiation and growth of cracks should be predictable from the results of quantitative microstructural and fractographic analysis. Composition, manufacturing technology and heat treatment all affect microstructural evaluation. This work focuses on the relations between microstructural parameters changed by varying the alloy composition, microscopic fracture mechanisms and resultant fracture toughness of overaged 7000 alloy plates used as aircraft components.

2. Experimental procedure

Three industrially produced alloys with compositions (in mass%): Al-7.45Zn-2.47Mg-1.53Cu-0.25Mn-0.17Cr-0.15Zr-0.11Si-0.12Fe (Alloy 1), Al-7.30Zn-2.26Mg-1.55Cu-0.29Mn-0.18Cr-0.13Zr-0.09Si-0.16Fe (Alloy 2) and Al-7.65Zn-2.26Mg-1.55Cu-0.25Mn-0.18Cr-0.11Zr-0.11Si-0.26Fe (Alloy 3) were supplied as uniaxially hot-forged pancake-type plates in T73 condition. They contain several types of SP particles, which are: (a) coarse irregular intermetallic phase (IMP) particles, which are clustered along the direction of the prevailing deformation. Most of these particles are unsoluble $(Cu,Fe,Mn)Al_3$ and Al_7Cu_2Fe phases, Fig. 1a. Their volume fraction and size vary with the Fe content. The soluble Mg_2Si, η-$Mg(Zn,Cu,Al)_2$ and S-$CuMgAl_2$ phases are not present in large amounts. (b) Round intragranular η precipitates with an average diameter of ~ 0.55 μm (arrowed in Fig. 1b). (c) Rectangular or elliptical $Al_{18}Cr_2Mg_3$ and $Al_{20}Mn_3Cu_2$ dispersoids with a length of ~ 100 nm and a width of ~ 40 nm, on which nucleated the quench-induced η-$MgZn_2$ precipitates reaching an average size of ~ 40 nm, Figs. 1b and c. (d) Elliptical quench-induced η precipitates being ~ 60 nm in length and ~ 20 nm in the short axis, which are present along the grain boundaries (arrowed in Fig. 1c). (e) Strengthening η precipitates much smaller than inter- and intragranular precipitates formed during quenching. Details of the microstructure assessment are given elsewhere[5].

To evaluate fracture micromechanisms, the L-R oriented compact-tension (CT) specimen fracture surfaces formed in a plane-strain fracture toughness test were examined using a scanning electron microscope (SEM). Before the K_{Ic} was determined in accordance with ASTM E399, a precracking stage was performed. The fractographic observations were made in the central region of the plastic zone ahead of the fatigue precrack. Quantitative description of fractures was performed using a profilometry method. The length of fracture profile disclosed on metallographic specimen perpendicular to an average fracture plane and profile fragments occupied by the individual IMP particles were measured using an image analyser operating on-line with the optical microscope (OM). These measurements enable to determine the following quantitative fractographic parameters: linear roughness parameter, R_L, surface roughness parameter, R_S, and phase dominance factor, ξ. The linear fraction, $L_{L(IMP)}$, and size, $L_{(IMP)}$, of coarse IMP particles were estimated on plane sections by linear-intercept method.

3. Results and discussion

The SEM observations reveal that all fracture surfaces are of the ductile type, Figs. 2a and b. Large voids, referred to as primary voids, always initiated at the coarse Fe-rich and Mg_2Si particles. Their fracture or decohesion occur in the first stages of plastic flow[5].

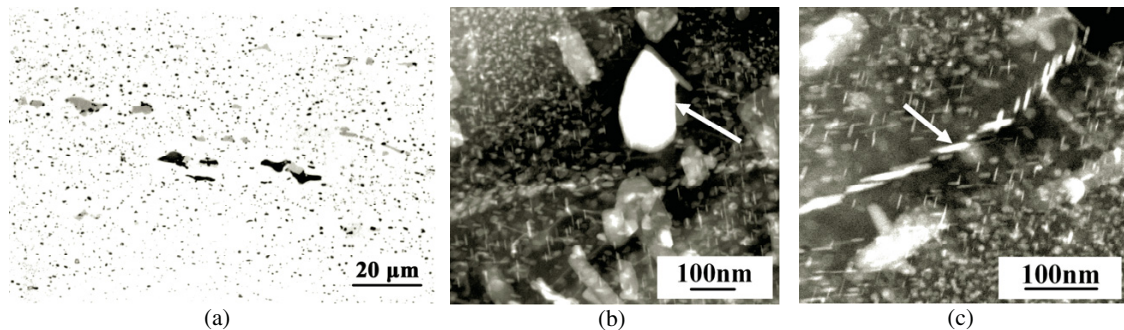| (a) | (b) | (c) |

Fig. 1. OM (a) and transmission electron (b, c) micrographs showing various SP particles.
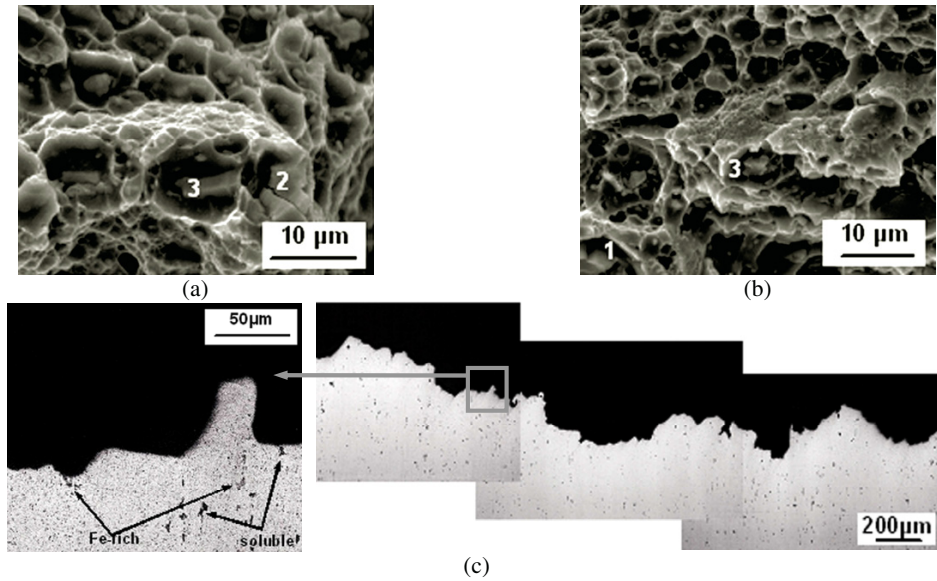
Fig. 2. SEM micrographs showing fracture surfaces (a, b) and characteristic fragment of fracture surfaces of Alloy 1 observed by OM (c). Phases: 1- Mg_2Si, 2-$(Cu,Fe,Mn)Al_3$, 3-Al_7Cu_2Fe.

Table 1. Results of microstructural and profilometric analysis along with fracture toughness data.

Perimeter	Meaning	Alloy		
		1	**2**	**3**
R_S^*	ratio of true surface area to its projected area	1.81	1.56	1.27
R_L	ratio of total length of profile to its projected length	1.64	1.44	1.21
$L_{L(Fe\text{-}rich)p}$ (%)	linear fraction of unsoluble Fe-rich phases on profile	0.304	1.470	3.140
$L_{L(soluble)p}$ (%)	linear fraction of soluble phases on profile	0.315	0.148	0.314
$L_{L(IMP)p}$ (%)	linear fraction of all IMP on profile	0.619	1.619	3.456
$L_{(Fe\text{-}rich)}$ (μm)	average size of Fe-rich particles in microstructure	2.00	1.99	2.43
$L_{(soluble)}$ (μm)	average size of soluble particles in microstructure	1.66	1.49	1.79
$L_{L(Fe\text{-}rich)}$ (%)	linear fraction of Fe-rich phases in microstructure	0.227	0.357	0.590
$L_{L(soluble)}$ (%)	linear fraction of soluble phases in microstructure	0.284	0.142	0.266
$L_{L(IMP)}$ (%)	linear fraction of all IMP in microstructure	0.511	0,499	0.856
$\xi_{(Fe\text{-}rich)}^{**}$	Fe-rich phases dominance factor	1.34	4.12	5.32
$\xi_{(soluble)}^{**}$	soluble phases dominance factor	1.11	1.04	1.18
$\xi_{(IMP)}^{**}$	unsoluble and soluble IMP dominance factor	1.21	3.24	4.04
K_{Ic} (MPa√m)	plane-strain fracture toughness	43.2	40.9	37.7

* $R_S = (4/\pi) (R_L - 1) + 1$

** $\xi = L_L^{profile}/L_L^{structure}$, where $L_L^{profile}$ is linear fraction of coarse particles on profile and $L_L^{structure}$ is the linear fraction of coarse particles in microstructure

Growth of the primary voids is more or less pronounced depending on the number of void initiation sites. Numerous microvoids, associated with dispersoid and other medium-sized particles, accelerate the onset of the void coalescence process. The presence of ridges and smaller, shallow voids clustered in locally very smooth zones initiating on coarse precipitates suggests that fracture also proceeds by a ductile intergranular mechanism. From these observations, the fracture process is multimechanistic in nature. Two fracture modes predominate: coarse, primary voiding and microvoid-induced transgranular fracture through the grains. The controlling micromechanism varies with alloy purity. The extent of coarse voiding increases with the increase of the (Fe+Si) impurity level and in turn the fraction and size of the coarse Fe- and Si-rich particles. Consequently, a transition from predominantly transgranular fracture to principally coarse voiding occurs, leading to a decrease in the fracture development and fracture toughness degradation.

The most developed surface is characteristic of the fracture of most pure alloy, Alloy 1, showing highest toughness, Fig. 2c. This is proved by the result of a quantitative profile evaluation. As can be seen from Table 1, the K_{Ic} value is directly proportional to both roughness parameters: R_L and R_S. Description of the fracture surface by these parameters permits us to estimate the extent of the first fracture event, *i.e.*, nucleation, growth and coalescence of voids at coarse IMP particles. Examples of particle cracks on the fracture surface is presented in Fig. 2c. Most of these particles are $(Cu,Fe,Mn)Al_3$ and Al_7Cu_2Fe phases. It appears, therefore, that when the Fe content is reasonably high, the fracture is dominated by particle cracking damage. That the phenomenon of crack initiation and propagation is fostered by coarse Fe-rich particles is confirmed by their dominance factor $\xi_{(Fe-rich)}$, which is higher than 1 for all the examined alloys and increases with the increase of impurity content. In contrast to this, the $\xi_{(soluble)}$ is almost constant. Its much lower value compared to $\xi_{(Fe-rich)}$ confirms that the dominant fracture mode and K_{Ic} level are strongly dependent on the Fe content.

4. Conclusions

The fracture process in overaged 7000 alloy plates is complex involving three micromechanisms: primary voiding at coarse IMP particles, ductile intergranular and microvoids-induced transgranular fracture. The extent of coarse voiding increases with the increase of impurity level and in turn the fraction and size of coarse Fe-rich particles, leading to a change in dominant fracture mode and toughness degradation. Profilometric analysis data are strictly correlated with a reduction in toughness. The value of $\xi_{(Fe-rich)}$ proves that crack initiation at $(Cu,Fe,Mn)Al_3$ and Al_7Cu_2Fe particles is a critical step in the fracture process.

Acknowledgements

References

1. Dumont D, Deschamps A, Brechet Y. On the relationship between microstructure, strength and toughness in AA7050 aluminum alloy. *Mater Sci Eng A* 2003;**356**:326-36.

2. Kamp N, Sinclair I, Starink MJ. Toughness-strength relations in the overaged 7449 Al-based alloy. *Metall Mater Trans A* 2002;**33A**:1125-36.

3. Deshpande NU, Gokhale AM, Denzer DK, Liu J. Relationship between fracture toughness, fracture path, and microstructure of 7050 aluminum alloy: Part I. Quantitative characterization. *Metall Mater Trans A* 1998;**29A**:1191-201.

4. Dumont D, Deschamps A, Brechet Y. A model for predicting fracture mode and toughness in 7000 series aluminium alloys. *Acta Mater* 2004;**52**:2529-40.

5. Cvijović Z, Rakin M, Vratnica M, Cvijović I. Microstructural dependence of fracture toughness in high-strength 7000 forging alloys. *Eng Fract Mech* 2008;**75**:2115-29.